DISCLAIMER

This work was performed under the auspices of the U. S. Department of Energy by the University of California, Lawrence Livermore National Laboratory under Contract No. W-7405-Eng-48.

UCRL-ID-145882

H_2O Outgassing in and its Effects on M9787 Silicone

L. N. Dinh, M. A. Schildbach, W. McLean II, B. Balazs, J. D. LeMay, M. Balooch

September 1, 2001

U.S. Department of Energy

Lawrence
Livermore
National
Laboratory

H_2O outgassing in and its effects on silica-filled polysiloxane

L. N. Dinh, M. A. Schildbach, W. McLean II, R. S. Maxwell, B. Balazs,

J. D. LeMay, and M. Balooch

Chemistry and Materials Science

Lawrence Livermore National Laboratory, Livermore, CA

ABSTRACT

Temperature programmed desorption (TPD) was performed on M9787 silicone, Cab-O-Sil-M-7D (fumed) and Hi-Sil-233 (precipitated) silica particles that had been annealed to 460 K for 24 hours then exposed to different moisture levels. Our results suggest that moisture desorption and adsorption in M9787 can be approximated by the interaction of its silica contents (Cab-O-Sil-M-7D and Hi-Sil-233) with moisture. Our experimental data also reveal that, in general, as heat-treated silica particles are exposed to moisture, chemisorbed states, then physisorbed states are gradually filled up in that order. However, there seems to have some rearrangement of bonds as moisture desorbs or absorbs on the surfaces of the silica particles. Nanoindentation was also performed on M9787 silicones that were simultaneously pumped down to a few hundred Pa of residual pressure at room temperature. Our data shows that the removal of physisorbed water in M9787 has none or reversible little effect on the mechanical properties of M9787.

Keywords: Silica, polymer, water outgassing, temperature programmed desorption.

I. INTRODUCTION

A family of silicone used by the U.S. Department of Energy is composed of polysiloxane gumstock (67.6 wt. %), fumed silica filler Cab-O-Sil M-7D (21.6 wt. %), precipitated silica filler Hi-Sil 233 (4 wt. %), and processing aid, chemically an ethoxy endblocked polysiloxane (6.8 wt. %). In this report, we also refer to these silicones as silica-filled polymers or silica filled polysiloxanes. Silica occupies ~ 25.6 wt. % in these silicones, and silica surfaces are well known to have a good affinity for water adsorption. Absorbed water may play an important role on the bonding between SiO_2 particles and the silicone matrix. The outgassing of water may change the nature of the silica/polymer bonding, even possibly the mechanical behavior of the materials. It may also present a compatibility issue in sealed systems containing these types of silicones over a long period of time at room or slightly elevated temperatures. In a previous report,[1] we have presented data on water outgassing from as-received fumed silica particles,Cab-O-Sil-M-7D, and precipitated silica particles, Hi-Sil-233. In order to clearly understand the mechanism of H_2O absorption and outgassing in M9787, we report, in this paper, experimental kinetic results on the desorption and absorption of water in M9787 silicone and both types of silicas which had been heat-treated then reexposed to different moisture levels. We will also present our results on the effect of pumping away physisorbed water on the mechanical properties of M9787 by nanoindentation.

II. MATERIALS and METHODS

Pre-weighted thin (300 μm) M9787 silicones or small amounts (0.004-0.009 g) of Cab-O-Sil-M-7D or Hi-Sil-233 silica powders were enveloped in Platinum (Pt) envelopes

with a dimension of 1 cm × 1 cm. The side of the envelopes facing the mass-spectrometer were perforated with holes which added up to ~ 0.75 cm^2. Each envelope was held fixed to a sample holder by ways of three mechanical clamps and transferred into an ultrahigh vacuum (UHV) chamber with a base pressure of 10^{-6} Pa (4 x 10^{-7} Pa in the detector chamber) through a differentially pumped load lock. The pressures in the various parts of the chamber were monitored with ion and baratron gases. A type K thermocouple was inserted in between the Pt envelope surface and a clamp holding the envelope for temperature measurement. The samples were heated from the back sides by passing currents through a Tungsten coil located 2 mm behind the samples. This tungsten coil was used for both annealing and TPD works. The detector chamber is equipped with a quadrupole mass spectrometer (QMS) and has been described in detail elsewhere.[2] Low level moisture re-exposures were perfomed by introducing H_2O vapor from a water reservoir into the TPD chamber with the gate valve connecting the chamber with the pumping system closed.

The techniques for TPD data analysis employed in this report have previously been published.[1,3] For studying the effects of H_2O outgassing on the mechanical properties of M9787, we have modified a vacuum chamber to house a Hysitron nanoindenter operated by a Digital Nanoscope III atomic force microscopy (AFM) controller. The vacuum chamber was pumped by liquid nitrogen pumps to a few hundreds Pa (as measured by a convectron gauge) and maintained over various lengths of time. Prior to starting nanoindentation works, we back-filled the chamber with Ar to a few ten thousands of Pa to avoid arching of the electronic components in the nanoindenter head. Measurement of the nanoindenter's tip radius was performed with quartz (Young modulus E_r = 69.6 GPa).

The procedure for this process was outlined by Hysitron and is repeated here for clarity. In Fig. 1, we show the projected area of a spherical tip onto a sample to be indented. In this picture, h is the distance from the tip end to the unperturbed sample surface (or the sample surface outside the indented area) at the deepest tip penetration location during a particular nanoindentation process, R is the radius of the projected area of the spherical tip onto the sample, and r is the radius of the nanoindenter spherical tip.

The projected area is given by:

$$A = \pi R^2 \tag{1}$$

But: $R^2 = r^2 - (r-h)^2$ (2)

From (1) and (2):

$$A = \pi h(2r - h) \tag{3}$$

The contact area of the indent is found using the standard modulus equation:

$$A = \frac{4S^2}{\pi E_r{}^2} \tag{4}$$

A force vs. indentation depth curve is obtained during nanoindentation. The slope of the unloading portion of the curve during the early stage of the tip withdrawal process coresponds to the contact stiffness,S. This is illustrated in Fig. 2 for a nanoindentation on a quartz surface with a maximum force of 5000 μN.

With E_r = 69.6 GPa and known S, an A vs. h plot can be obtained when performing nanoindentations with different maximum forces. The tip radius can be obtained by fitting the A vs. h plot with equation (3).

In Fig. 3, we show the curve fitting of experimentally obtained values of A and h with equation (3) to obtain the radius of curvature for the tip which was r = 37.43 μm for all

nanoindentations reported here. The inset show the simulated shape of A vs. h using the curve fitted value of r for values of h up to 30 μm. Once, the tip radius is known, nanoindentation on sample whose Young modulus is to be measured can start. But care has to be taken so that the forces employed during nanoindentation do not produce h that is much greater than those employed in calibrating the tip radius. Reduced Young modulus of the sample under studied can be directly read out from:

$$E_r = \frac{2S}{\pi[h(2r-h)]^{0.5}} \tag{5}$$

III. RESULTS & DISCUSSION

The effects of desorbing physisorbed H_2O on the mechanical properties of M9787

Fig. 4 shows the force vs. indentation depth for a location on M9787 before any pumping action. M9787 silicone is much softer than silica and so it took only 15 μN to indent the silicone to a depth of ~ 220 nm. It is then expected that the Young modulus associated with M9787 is many orders of magnitude less than that associated with quartz. In this experiment, we did indentations at five locations labeled: A, B, C, D, E on M9787 as a function of pumping time up to 18 hours at room temperature. This is enough to pump out only physisorbed water in M9787.[1] Table I summarizes the variations in the values of Young modulus obtained by nanoindentations of M9787 at A, B, C, D and E as a function of pumping time. Within an error bar of ~ 15 %, the values of Young modulus at 4 out of 5 points (A, B, C and D) appeared to stay constant. The Young modulus at only 1 out of 5 points (E) reduced by ~ 30 % as physisorbed water was pumped out. The differences in the mechanical behavior of these points might be due to a non-uniform distribution of silica in the polymer matrix. When the gate valve to the pumping system

was closed and air was re-introduced into the chamber, the original values of E_r before pumping were obtained again. So, we conclude that losing physisorbed water had very little effect on the mechanical properties of M9787 (if any) and that any change in the measured properties was also reversible. The potential for mapping of silica distribution in the M9787 silicone by AFM related techniques, such as nanoindentation mapping or phase measuring mode on slices of M9787 cut by our newly obtained microtoner at liquid nitrogen temperature, are being developed.

Environmental changes	Fractional variation in E_r at point A	Fractional variation in E_r at point B	Fractional variation in E_r at point C	Fractional variation in E_r at point D	Fractional variation in E_r at point E
Pumping time (0 hour)	1	1	1	1	1
Pumping time (8 hours)	1.054	0.8	0.862	1.05	0.71
Pumping time (10.5 hours)	1.009	0.913	0.842	1.06	0.69
Pumping time (17.5 hours)	1.072	0.928	0.829	1.13	0.67
Re-exposed to air	0.9	1.021	1.131	1.15	1.033

TPD of Cab-O-Sil-M-7D and Hi-Sil-233 silicas and M9787 subjected to different moisture environments

Fig. 5(a) and (b) show H_2O TPD spectra from as-received Cab-O-Sil-M-7D and Hi-Sil-233 at a ramping rate of 0.1 K/s respectively. These spectra have been background

substracted from an essentially flat response of the Pt foil envelope. Each spectrum can be seen to consist of many separate desorption curves as reported previously.[1] These peaks are associated with physisorbed and chemisorbed water from silica surfaces.[4,5] The technique of iterative regression analysis reported earlier was employed in the decomposition of the TPD spectra presented in this paper into constituent desorption curves.[1,3] The relative ratios of the areas occupied by these desorption curves are: curve I/curve II/curve III/curve IV = 1/41.7/18.2/21.8 for Cab-O-Sil-M-7D and curve I/curve II/curve III/curve IV = 1/24.6/20.4/8.4 for Hi-Sil-233. The kinetic parameters such as activation energy (E), pre-exponential factor (υ) and desorption order (n) associated with these desorption curves are summarized in table I and II below.

	Curve I	**Curve II**	**Curve III**	**Curve IV**	**Curve V**
n	1	1	2	2	2
E (kJ/mol)	68.6	25.7	111.6	133.5	>150
υ (s^{-1})	1.35×10^{8}	5.63×10^{-1}	1.42×10^{7}	2.28×10^{7}	$>10^{8}$

Table I: The values of E_d and ν for the different decomposition curves of an as-received Cab-O-Sil-M-7D.

	Curve I	**Curve II**	**Curve III**	**Curve IV**	**Curve V**
n	1	1	2	2	2
E (kJ/mol)	57.6	37.5	102	149.5	>155
υ (s^{-1})	1.33×10^{6}	4	2.31×10^{5}	5.97×10^{7}	$>10^{8}$

Table II: The values of E_d and ν for the different decomposition curves of an as-received Hi-Sil-233.

Note that in both tables, the H_2O physisorbed (n =1) curves II have lower activation energies and lower pre-exponential factors than curves I even though the peak desorption temperatures for curves II are higher than those for curves I (see Fig. 5). One sees that curves II are very broad around the peak desorption temperatures while curves I are much more narrower. So, it is clear that activation energy or peak desorption temperature alone cannot uniquely describe a desorption process. One needs to specify all four parameters: n, E, υ and β (heating ramp rate) to uniquely specify a TPD desorption curves according to the desorption rate equation:[1]

$$-\frac{d\sigma}{dt} = \frac{\upsilon}{\beta}\sigma^n \exp\left(-\frac{E}{RT}\right) \tag{6}$$

where σ is the ratio of concentration of H_2O on the surface of the silica particles at time t to the initial H_2O surface concentration at t = 0.

In Fig. 6, the thick solid line represents the experimentally measured desorption rate of 0.0475 gram (g) of M9787 (containing ~ 0.01026g and 0.0019g of Cab-O-M-7D and Hi-Sil-233 silica particles respectively) wrapped inside a 1 cm^2 Pt envelope (with holes all over the surface of the envelope facing the mass spectrometer). This sample was ramped to 460 K at 0.1 K/s and held at 460 K for about 1500 minutes. Note that due to the degradation of M9787 at around 550K, we did not heat M9787 above 500K. The dash line represents the simulated isothermal desorption curve corresponding to 0.01026g of Cab-O-Sil-M-7D and 0.0019g of Hi-Sil-233 silica particles wrapped inside a similar envelope and subjected to a similar heat-treatment according to the kinetic parameters obtained in tables I and II. More details of the simulation is given in the Appendix A. The initial desortion rate at 460K for M9787 is about 26% lower than that for the simulated isothermal desorption curve for 0.01026g of Cab-O-Sil-M-7D and 0.0019g of Hi-Sil-233. But this was within calibration error for our mass spectrometer system in going from one sample to another. The maximum calibration error in our system had been as high as 50% (upon breaking the vacuum for changing parts) even though error of ~ 25% or less were more frequently encountered. In the long time limit, the two isothermal desorption curves behave very similarly, but within the first 200 minutes of heating at 460K, there was less water coming out from the 0.0475g of M9787 than from the sample containing an equivalent amount of silica particles. This suggests that when silica particles were

embedded in the M9787 during production, some portion of the H_2O molecules and/or Si-OH bonds on the surfaces of silicas were actively used as bonding between silicas and the polymer matrix resulting in less H_2O outgassing from M9787 than from its constituent silica content when the latter was not in the polymer matrix. Nevertheless, the difference in the two isothermal curves might very well be due to our high error margins in the calibration of the mass spectrometer and sample to sample variation. Current efforts to improve the precision and accuracy of the calibration procedure for our mass spectrometer and to assess sample to sample variation are under way. The wt. % of water removed over 1500 minutes of annealing at 460K are ~ 0.03 to 0.04 and 0.09 to 0.13 for the M9787 and the equivalent silica amounts respectively. It is noted that the above derived H_2O wt. % were due to the removal of H_2O corresponding to the portion of curves II in Fig. 5 with T > 460K and some portion of curves III during the 1500 minutes annealing at 460K. The actual H_2O wt. % removed should be roughly a factor of two higher if one includes the amount of H_2O desorbed during the linear heating ramp from 300K to 460K. The total wt. % of H_2O including all physisorbed and chemisorbed water (see Fig. 5) should be a factor of 3 or 4 higher than the numbers presented above.

Fig. 7(a) and (b) show H_2O TPD spectra from Cab-O-Sil-M-7D and Hi-Sil-233, that had been heat-treated at 460K for 24 hours then re-exposed to room air at 50% relative humidity (RH) for 15 minutes, at a ramping rate of 0.25 K/s respectively. Each of these spectra can also be decomposed into many separate desorption curves. The relative ratios of the areas occupied by these desorption curves are: curve I/curve II/curve III = 1/6.6/7.7 for Cab-O-Sil-M-7D and curve I/curve II/curve III/curve IV/curve V = 1/2.6/5.6/12.7/7.4 for Hi-Sil-233. The kinetic parameters associated with these desorption curves are summarized in table III and IV below.

	Curve I	Curve II	Curve III	Curve IV
n	1	2	2	2
E (kJ/mol)	35.1	74.2	106.3	153.5
υ (s^{-1})	59.51	3.79×10^4	6.05×10^5	5.62×10^7

Table III: The values of E_d and ν for the different decomposition curves of Cab-O-Sil-M-7D that had been heat-treated at 460K for 24 hours then re-exposed to air at 50% RH for 15 minutes.

	Curve I	Curve II	Curve III	Curve IV	Curve V
n	1	1	1	2	2
E (kJ/mol)	66.2	26.5	72.2	108	145.4
υ (s^{-1})	4.80×10^7	4.30	3.69×10^4	6.40×10^6	3.51×10^8

Table IV: The values of E_d and ν for the different decomposition curves of Hi-Sil-233 that had been heat-treated at 460K for 24 hours then re-exposed to air at 50% RH for 15 minutes.

Comparing Fig. 5 with Fig. 7, one can see that the spectra of silica particles that had been heat-treated at 460K for 24 hours and then re-exposed to room air at 50% RH for 15 minutes have much less physisorbed waters. This is particularly obvious for Cab-O-Sil-M-7D. There also appears to be some differences in the shapes of the TPD spectra in the chemisorbed region. This might have been due to some rearrangement of SiOH bonds on the surfaces of silica when H_2O molecules were added or removed.

In Fig. 8, the thick solid line represents the experimentally measured desorption rate, at 460K, of the same 0.0475 g of M9787 as in Fig. 6 but after 24 hours of heat-treatment at 460K followed by re-exposure to room air at 50% RH for 15 minutes. The dash line represents the simulated isothermal desorption curve corresponding to 0.01026g of Cab-O-Sil-M-7D and 0.0019g of Hi-Sil-233 silica particles subjected to the same heat

and moisture treatment as the M9787 sample. The simulation was based on the kinetic parameters obtained in tables III and IV (see Appendix A). Similar to Fig. 6, the initial desortion rate at 460K for M9787 is about 25% lower than that for the simulated isothermal desorption curve for 0.01026g of Cab-O-Sil-M-7D and 0.0019g of Hi-Sil-233. Again, in the long time limit, the two isothermal desorption curves behave very similarly, but within the first 200 minutes of heating at 460K, there was less water coming out from the 0.0475g of M9787 than from the equivalent silica sample. This was probably due to the fact that a portion of the silica surfaces have been tied up in the bonding with the polymer matrix and so there were less sites for accomodating new arriving H_2O molecules during the moisture re-exposure time. The wt. % of water removed over 1500 minutes of annealing at 460K are 0.011 and 0.044 for the M9787 and the equivalent silica amounts respectively.

Since the H_2O desorption rates for the equivalent silica sample have consistently been higher than those of the corresponding M9787 under different heating and moisture exposure conditions, water outgassing from Cab-O-Sil-M-7D and Hi-Sil-233 can be regarded as the upper limit for water outgassing in M9787.[6] This is so when considering that the fractional amount of water outgassing at 460K for 1500 minutes is comparable with the amount of water outgassing at room temperature over 100 years [see Fig 9 (a) and (b) for desorption curve II in Fig. 7(a) at 300K and 460K]. The equations used for the simulation in Fig. 9 were derived in ref. 1 and are presented in appendix A of this report.

Figs. 10(a) and 11(a) show TPD spectra of Cab-O-Sil-M-7D and Hi-Sil-233 that had been heat-treated at 460K for 24 hours then re-exposed to 2.1 Pa and 7.6 Pa of moisture for 24 hours respectively. The linear heating rates were 1 K/s for the Cab-O-Sil-M-7D sample 0.25 K/s for the Hi-Sil-233 sample. Figs. 10(b) and 11(b) correspond to TPD spectra of Cab-O-Sil-M-7D and Hi-Sil-233 that had been heat-treated at 460K for 24 hours and then cooled down in the vacuum chamber at 10^{-6} Pa prior to TPD. The linear heating rate for both samples were 0.25 K/s. These spectra were also composed of different desorption curves. The relative ratios of the areas occupied by these desorption curves are: curve I/curve II/curve III = 1/19.5/20.3 for the Cab-O-Sil-M-7D sample exposed to 2.1 Pa of moisture; curve I/curve II/curve III = 1/1.04/1.23 for the Cab-O-Sil-M-7D sample kept in vacuum; curveI/curveII/curveIII/curveIV/curve V =

1/3.03/2.90/18.4/20.04 for the Hi-Sil-233 sample exposed to 7.6 Pa of moisture; curveI/curveII/curveIII = 1/1.07/0.35 for the other Hi-Sil-233 sample. Due to a lack in reliable calibration data for the mass spectrometer for these particular samples, the units for the desorption rates are arbitrary in these spectra (they are on the same order of magnitude as those presented in Fig. 5 and 7 though). Fortunately, exact units are not necessary in deriving the kinetic parameters for these curves which are summarized in table V, VI, VII and VIII.

	Curve I	**Curve II**	**Curve III**	**Curve IV**
n	1	2	2	2
E (kJ/mol)	35.6	82.6	116.2	> 150
υ (s^{-1})	301	6.31×10^5	1.17×10^7	$> 10^8$

Table V: The values of E_d and ν for the different decomposition curves of Cab-O-Sil-M-7D that had been heat-treated at 460K for 24 hours then re-exposed to moisture at 2.1 Pa for 24 hours.

	Curve I	**Curve II**	**Curve III**	**Curve IV**
n	2	2	2	2
E (kJ/mol)	106	131.6	160	> 170
υ (s^{-1})	5.96×10^7	2.68×10^8	4.45×10^9	$> 10^{10}$

Table VI: The values of E_d and ν for the different decomposition curves of Cab-O-Sil-M-7D that had been heat-treated at 460K for 24 hours then cooled down to room temperature in the TPD chamber at 10^{-6} Pa of residual pressure.

	Curve I	Curve II	Curve III	Curve IV	Curve V	Curve VI
n	1	1	1	2	2	2
E (kJ/mol)	68.6	31.3	83.2	108	131	> 150
υ (s^{-1})	4.38×10^7	21.32	1.76×10^6	4.26×10^7	1.58×10^8	$> 10^9$

Table VII: The values of E_d and ν for the different decomposition curves of Hi-Sil-233 that had been heat-treated at 460K for 24 hours then re-exposed to moisture at 7.6 Pa for 24 hours.

	Curve I	Curve II	Curve III
n	2	2	2
E (kJ/mol)	108	137.4	>140
υ (s^{-1})	4.25×10^7	5.61×10^8	10^7

Table VIII: The values of E_d and ν for the different decomposition curves of Hi-Sil-233 that had been heat-treated at 460K for 24 hours then cooled down to room temperature in the TPD chamber at 10^{-6} Pa of residual pressure.

In comparing and contrasting Figs. 10 and 11 and tables VI and VIII, it is observed that the effect of annealing at 460K was to remove all physisorbed water and chemisorbed water with activation energy < 106-108 kJ/mol and pre-exponential factor > 4.25-5.96 × 10^7 s^{-1} . From Figs. 5, 7, 10 and 11 and tables I through VIII, it is seen that the effect of re-exposure of the heat-treated silica samples to moisture was to replenish depleted chemisorbed and physisorbed water on the silica surfaces more or less in that order. This is more clearly seen when we plot all of these spectra in the same plot as presented in Fig. 12(a) for Cab-O-Sil-M-7D and Fig. 12(b) for Hi-Sil-233. In comparison

with Cab-O-Sil-M-7D, previously heat-treated Hi-Sil-233 appeared to take up much more H_2O during re-exposure to moisture. It is also seen that as physisorbed or chemisorbed water was removed or added to the silica surfaces, there were rearrangements of the chemisorbed bonds, evidenced more clearly in the broadening of the chemisorbed states of Hi-Sil-233 at high levels of moisture. However, for the purpose of predicting the outgassing of these silica based materials, one is more concerned with the physisorbed and loose chemisorbed states. It is also noted after the heat-treatment at 460K for 24 hours, even the loosest chemisorbed states from Cab-O-Sil-M-7D and Hi-Sil-233 [curves I in Figs. 10(b) and 11(b)] are fairly stable against outgassing at room temperature over the next 100 years as can be seen in the simulations of Fig. 13.

IV. SUMMARY

We have performed TPD on M9787 silicone, Cab-O-Sil-M-7D and Hi-Sil-233 silica particles subjected to a variety of heat and moisture treatments. Our results suggest that water outgassing from Cab-O-Sil-M-7D and Hi-Sil-233 can be regarded as the upper limit for water outgassing in M9787. Unfortunately, large error margins in the calibration of our mass spectrometer and sample to sample variation somewhat undermine this statement. Current efforts to improve the precision and accuracy of the calibration procedure for our mass spectrometer and to assess sample to sample variation are under way. Our experimental data also reveal that, in general, as heat-treated silica particles are exposed to moisture, chemisorbed states, then physisorbed states are gradually filled up in that order. However, there seems to have some rearrangement of bonds as moisture desorbs or absorbs on the surfaces of the silica particles. Nanoindentation was also

performed on M9787 silicones that were simultaneously pumped down to a few hundred Pa levels of residual pressure at room temperature. Our data shows that the removal of physisorbed water in M9787 has none or reversible little effect on the mechanical properties of M9787. Current efforts in obtaining the SiO_2 distribution in the M9787 and the mechanical properties of M9787 when chemisorbed water is removed by AFM/nanoindentation related techniques are under way.

V. ACKNOWLEDGEMENT

This work was performed under the auspices of the U.S. Department of Energy by the University of California, Lawrence Livermore National Laboratory under contract No. W-7405-ENG-48.

VI. REFERENCES

1. L. N. Dinh, M. Balooch, J. D. LeMay, J. Colloid Interface Sci. **230**, 432 (2000).
2. L. N. Dinh, M. Balooch, J. D. LeMay, Desorption kinetics of H_2O, H_2, CO, and CO_2 from silica reinforced polysiloxane, UCRL-ID-135387, Lawrence Livermore National Laboratory.
3. K. H. Van Heek and H. Juntgen, Ber. Bunsenges. Physik. Chem. **72**, 1223 (1968).
4. J. B. Miller, H. R. Siddiqui, S. M. Gates, J. N. Russel, jr., J. T. Yates, jr., J. Chem. Phys. **87**, 6725 (1987).
5. V. M. Gun'ko, V. I. Zarko, B. A. Chuikov, V. V. Dudnik, Yu. G. Ptushinskii, E. F. Voronin, E. M. Paklov, A. A. Chuiko, Inter. J. Mass Spectrome. Ion Process. **172**, 161 (1998).
6. Similar TPD experiments on the filler for M9787 (M9787 without silicas) show water outgassing more than 2 orders of magnitude lower than those encountered in silicas and so the filler for M9787 will not be regarded as a source of moisture in M9787.

FIGURE CAPTIONS

Fig. 1: The projected area of a spherical tip onto a sample to be indented.

Fig. 2: Nanoindentation on a quartz surface with a maximum force of 5000 μN.

Fig. 3: Curve fitting of experimentally obtained values of A and h with equation (3) to obtain the radius of curvature for the tip, r. The inset show the simulated shape of A vs. h using the curve fitted value of r for values of h from 0 to 100 μm.

Fig. 4: Force vs. indentation depth for a location on M9787.

Fig. 5: TPD spectra of 0.004g of as-received Cab-O-Sil-M-7D (a) and 0.0054g of as-received Hi-Sil-233 at 0.1 K/s linear heating rate.

Fig. 6: Experimentally measured isothermal desorption rate of 0.0475g of M9787 (solid line) at 460K according to a linear ramp rate of 0.1 K/s and simulated desorption rate from 0.01026g of Cab-O-Sil-M-7D and 0.0019g of Hi-Sil-233 according to tables I and II (dash line).

Fig. 7: H_2O TPD spectra from Cab-O-Sil-M-7D (a) and Hi-Sil-233 (b), that had been heat-treated at 460K for 24 hours then re-exposed to room air at 50% relative humidity (RH) for 15 minutes, at a ramping rate of 0.25 K/s.

Fig. 8: Experimentally measured desorption rate, at 460K, of the same 0.0475 g of M9787 as in Fig. 6 but after 24 hours of heat-treatment at 460K followed by re-exposure to room air at 50% RH for 15 minutes (solid line) and simulated isothermal desorption curve corresponding to 0.01026g of Cab-O-Sil-M-7D and 0.0019g of Hi-Sil-233 silica particles subjected to the same heat and moisture treatment as the M9787 sample according to the kinetic parameters obtained in tables III and IV (dash line).

Fig. 9: Simulation of fractional water outgassing from curve II of Fig. 7(a) at 460K(a) and at 300K (b) as a function of time.

Fig. 10: Spectra of Cab-O-Sil-M-7D that had been heat-treated at 460K for 24 hours then re-exposed to 2.1 Pa of moisture for 24 hours (a) and of Cab-O-Sil-M-7D that had been heat-treated at 460K for 24 hours and then cooled down in the vacuum chamber at 10^{-6} Pa prior to TPD (b).

Fig. 11: Spectra of Hi-Sil-233 that had been heat-treated at 460K for 24 hours then re-exposed to 7.6 Pa of moisture for 24 hours (a) and of Hi-Sil-233 that had been heat-treated at 460K for 24 hours and then cooled down in the vacuum chamber at 10^{-6} Pa prior to TPD (b).

Fig. 12: Normalized TPD spectra of Cab-O-Sil-M-7D (a) and Hi-Sil-233 (b) subjected to different heat and moisture treatments.

Fig. 13: Simulation of fractional water outgassing from curves I of Figs. 10(b) and 11(b).

APPENDIX A:

The isothermal desorption rate at 460K according to a linear ramp rate of β (K/s) for 0.01026g of Cab-O-Sil-M-7D and 0.0019g of Hi-Sil-233 $= \sum_{i}^{j}\left[\frac{d\left\{\left(1-\sigma_{i,j}\right)A_{i,j}\right\}}{dt}\right]$ (with i: 0.01026g of Cab-O-Sil-M-7D, 0.0019g of Hi-Sil-233 and j: desorption curves I, II, III, IV,V...etc.). Here, $(1-\sigma_{i,j})$ is the fractional amount of H_2O released by the particular desorption curve described by i and j. $A_{i,j}$ is the area under the TPD desorption curve described by i and j (see Fig. 5) in the units of Pa.s (note that the relationship between t and T is: $T = T_o + \beta t$) at 460K. For example, $A_{i,j=1} = 0$ since after ramping up to 460K with a linear ramp rate of β, the desorption curves described by i and j = 1 have been completely desorbed (see Fig. 5).

$A_{i,j=2}$ are the areas under desorption curves (with a linear ramp rate of β) described by i and j = 2 corresponding to T > 460K. The formulae for calculating σ has been derived in a previous report[1] and are:

$$\sigma(t) = \exp\left\{-t\upsilon\, e^{-\frac{E}{RT}}\right\} \text{ for n = 1}$$

and

$$\sigma(t) = \frac{1}{1+t\upsilon\, e^{-\frac{E}{RT}}} \text{ for n = 2}$$

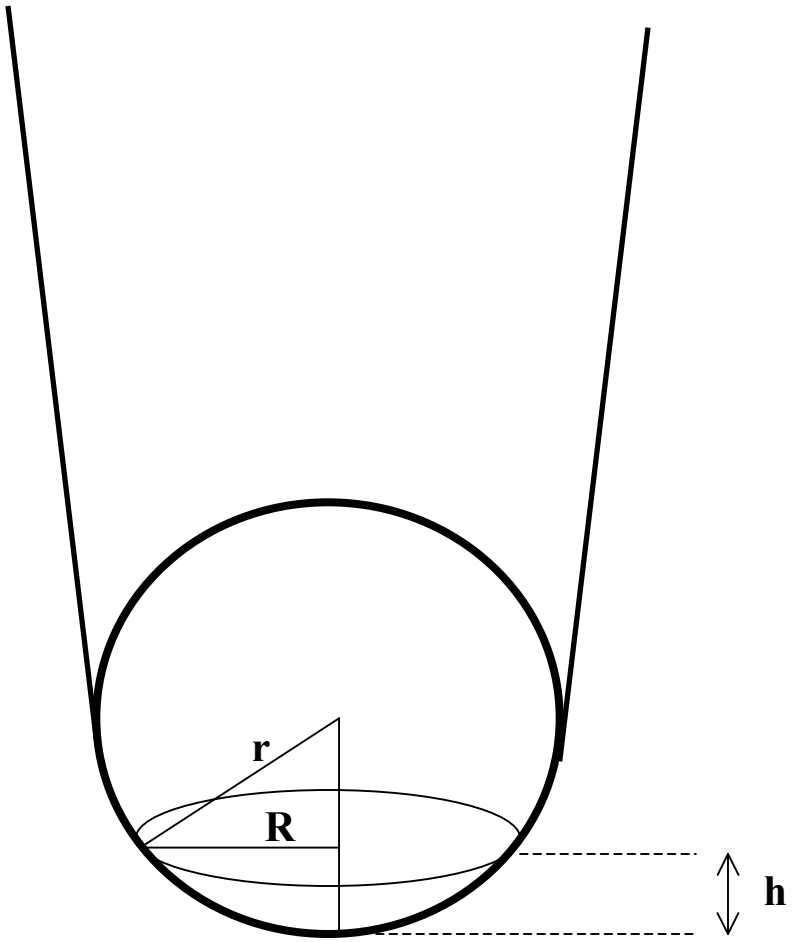

Fig. 1

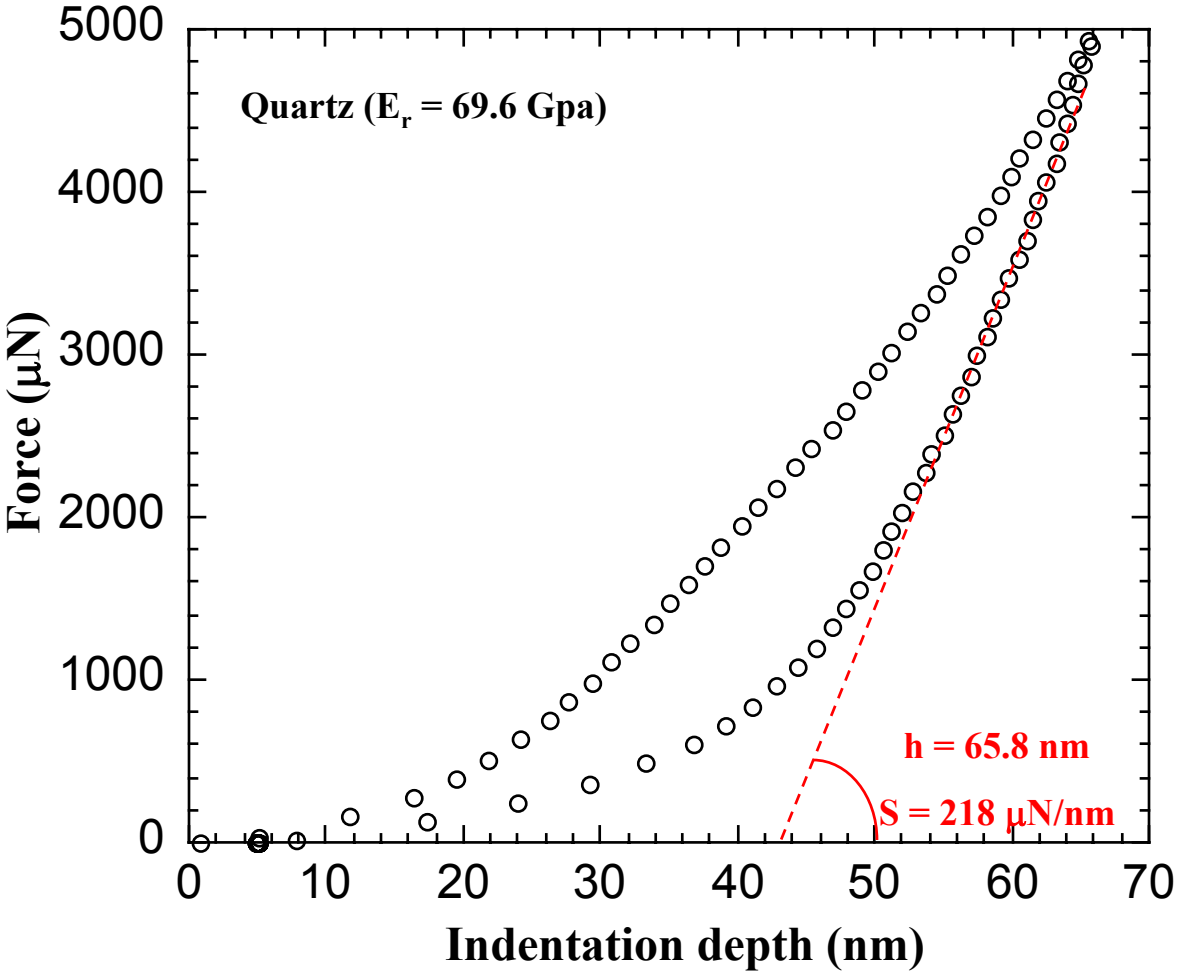
Quartz (E_r = 69.6 Gpa)
h = 65.8 nm
S = 218 μN/nm
Force (μN)
Indentation depth (nm)
0
1000
2000
3000
4000
5000
0
10
20
30
40
50
60
70

Fig. 2

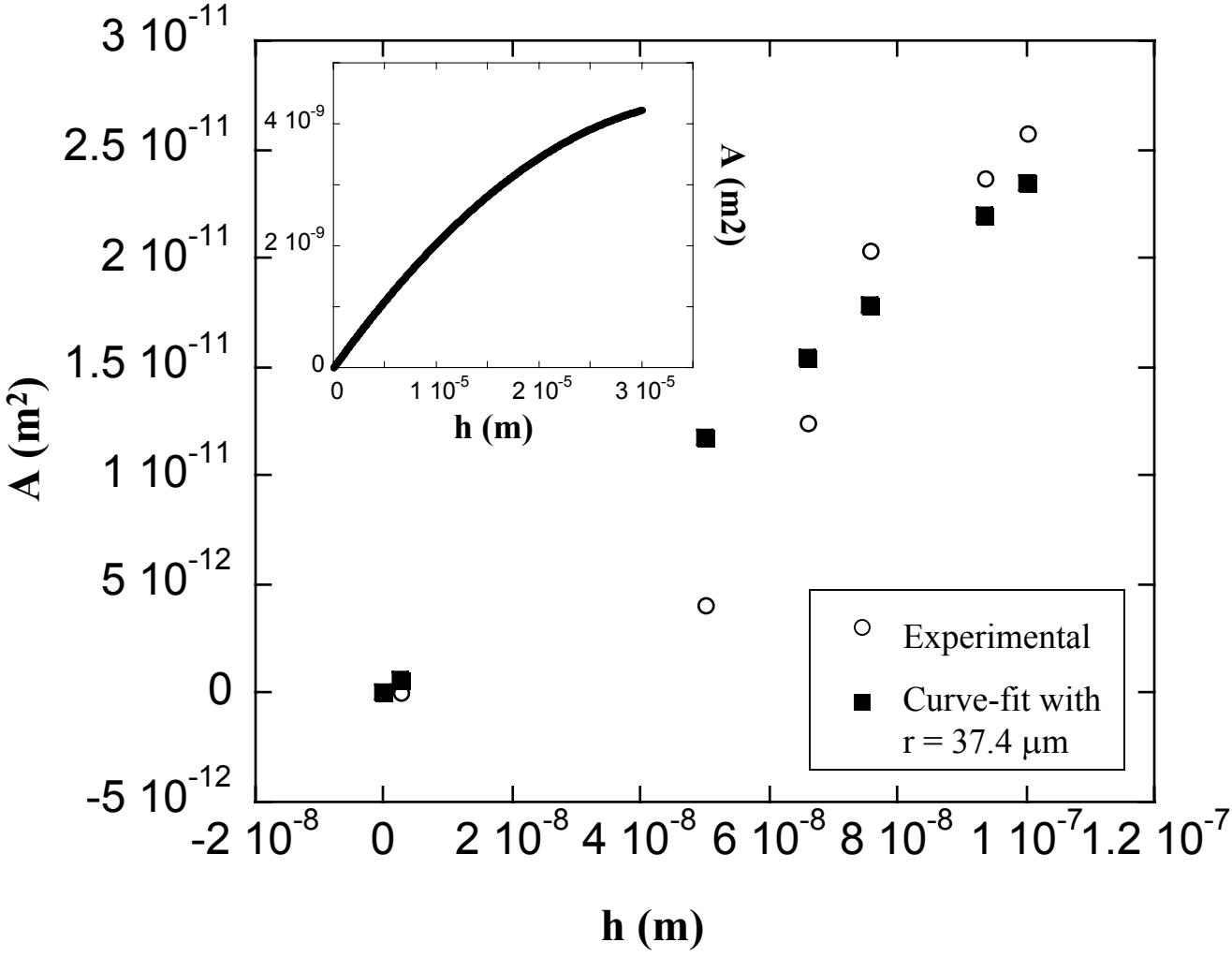
3 10^-11
2.5 10^-11
2 10^-11
1.5 10^-11
1 10^-11
5 10^-12
0
-5 10^-12
A (m²)
-2 10^-8
0
2 10^-8
4 10^-8
6 10^-8
8 10^-8
1 10^-7
1.2 10^-7
h (m)
Experimental
Curve-fit with
r = 37.4 μm
4 10^-9
2 10^-9
0
A (m2)
0
1 10^-5
2 10^-5
3 10^-5
h (m)

Fig. 3

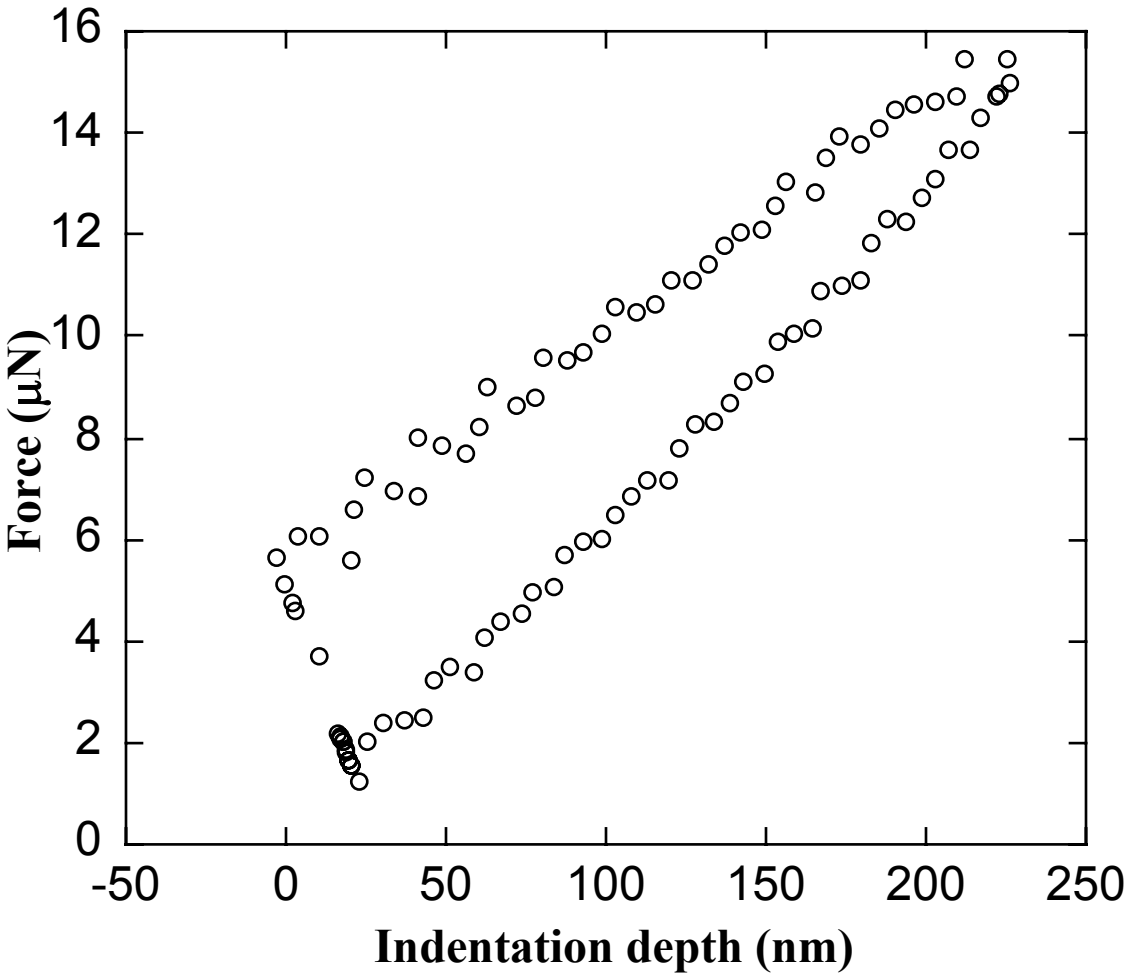
16
14
12
10
8
6
4
2
0
Force (μN)
-50
0
50
100
150
200
250
Indentation depth (nm)

Fig. 4

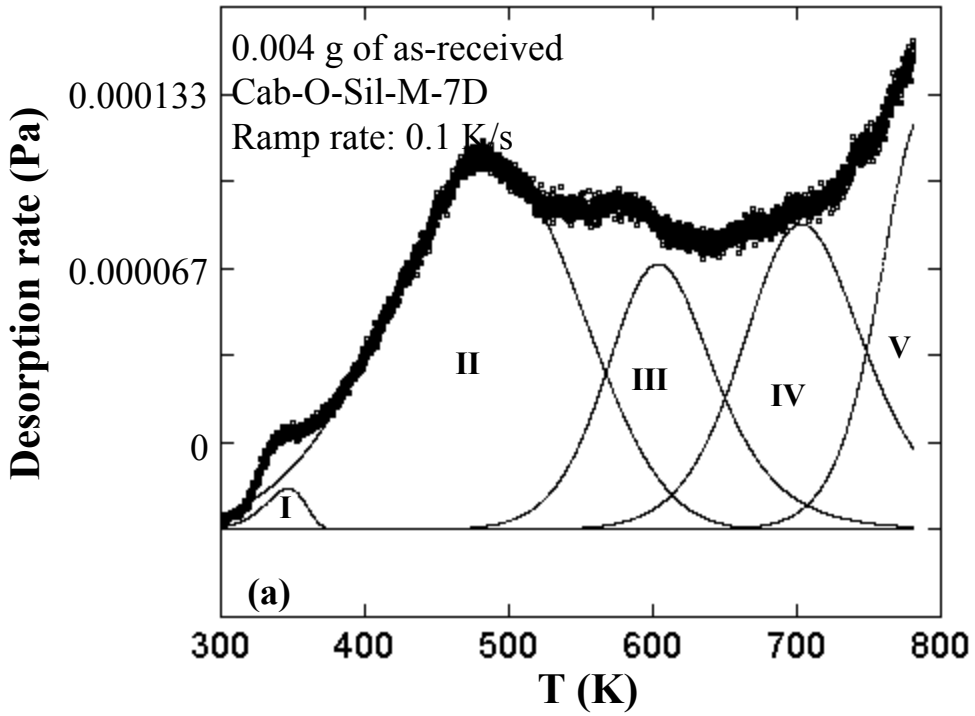
0.004 g of as-received
Cab-O-Sil-M-7D
Ramp rate: 0.1 K/s
0.000133
0.000067
0
Desorption rate (Pa)
I
II
III
IV
V
(a)
300
400
500
600
700
800
T (K)

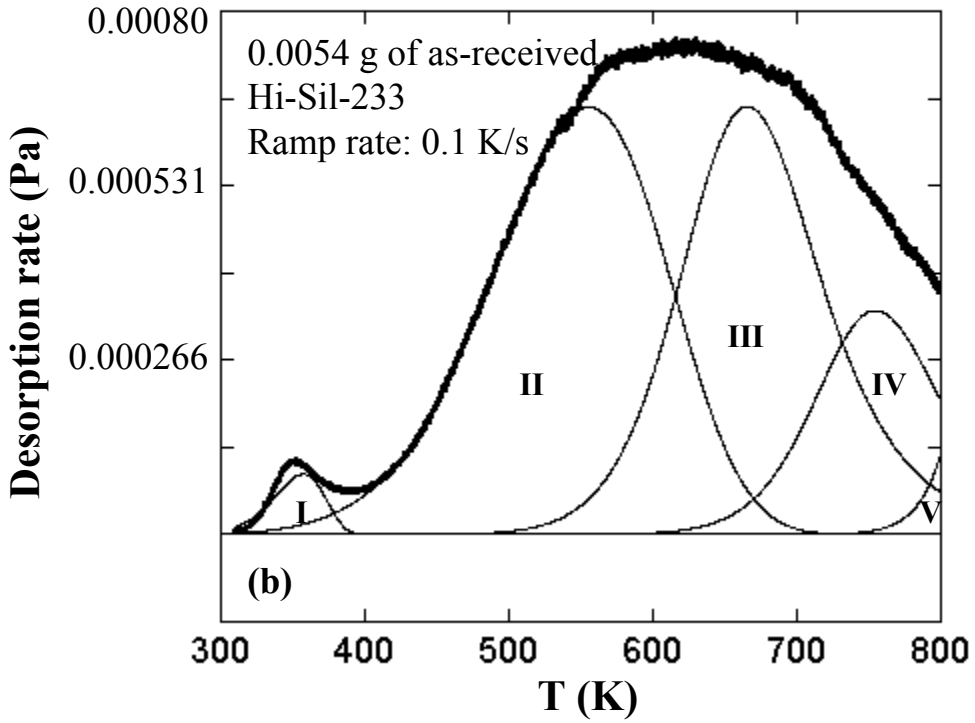
0.0054 g of as-received
Hi-Sil-233
Ramp rate: 0.1 K/s
0.00080
0.000531
0.000266
Desorption rate (Pa)
I
II
III
IV
V
(b)
300
400
500
600
700
800
T (K)

Fig. 5

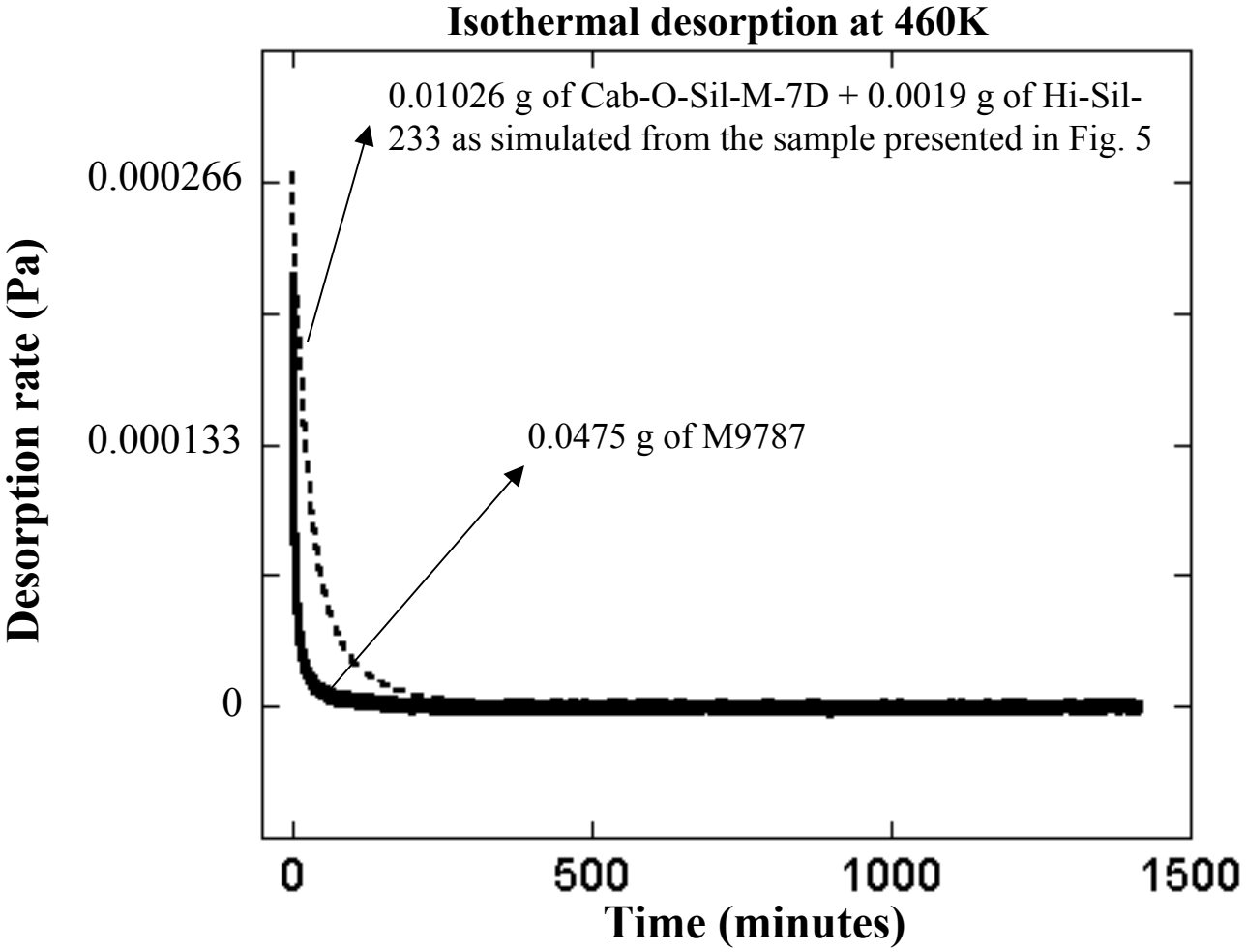
Isothermal desorption at 460K
0.01026 g of Cab-O-Sil-M-7D + 0.0019 g of Hi-Sil-233 as simulated from the sample presented in Fig. 5
0.0475 g of M9787
0.000266
0.000133
0
Desorption rate (Pa)
0
500
1000
1500
Time (minutes)

Fig. 6

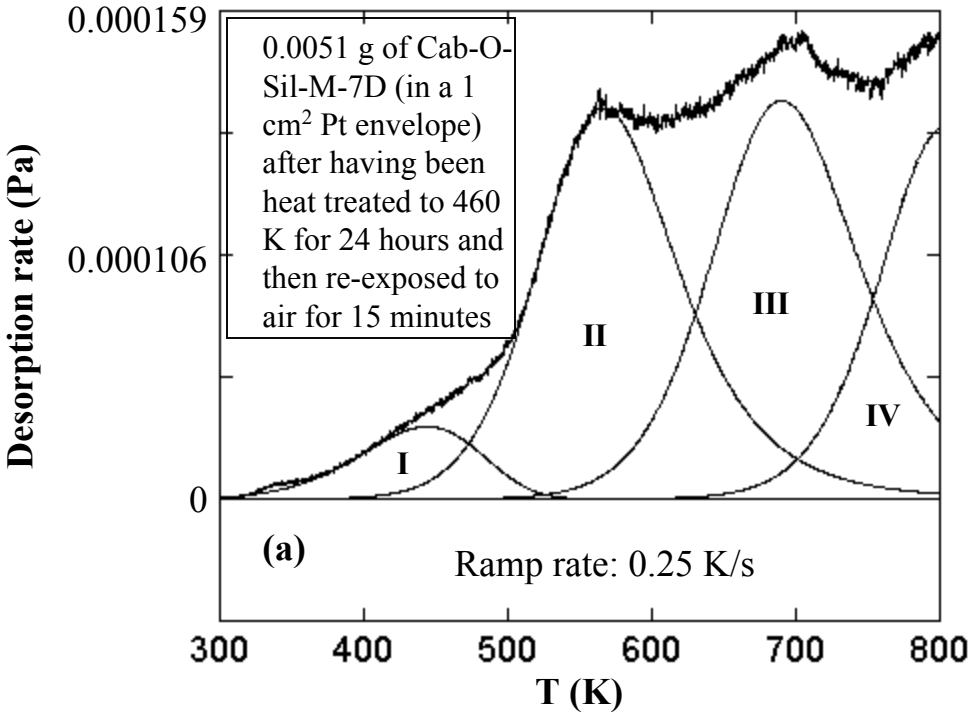
0.000159
0.000106
0
Desorption rate (Pa)
0.0051 g of Cab-O-Sil-M-7D (in a 1 cm2 Pt envelope) after having been heat treated to 460 K for 24 hours and then re-exposed to air for 15 minutes
I
II
III
IV
(a)
Ramp rate: 0.25 K/s
300
400
500
600
700
800
T (K)

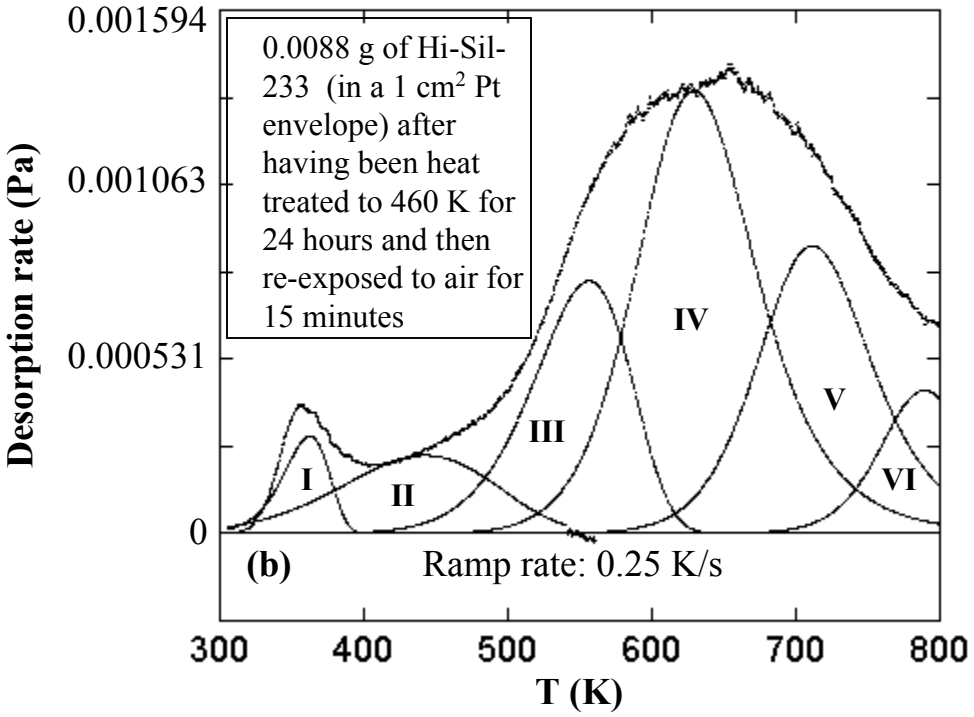
0.001594
0.001063
0.000531
0
Desorption rate (Pa)
0.0088 g of Hi-Sil-233 (in a 1 cm2 Pt envelope) after having been heat treated to 460 K for 24 hours and then re-exposed to air for 15 minutes
I
II
III
IV
V
VI
(b)
Ramp rate: 0.25 K/s
300
400
500
600
700
800
T (K)

Fig. 7

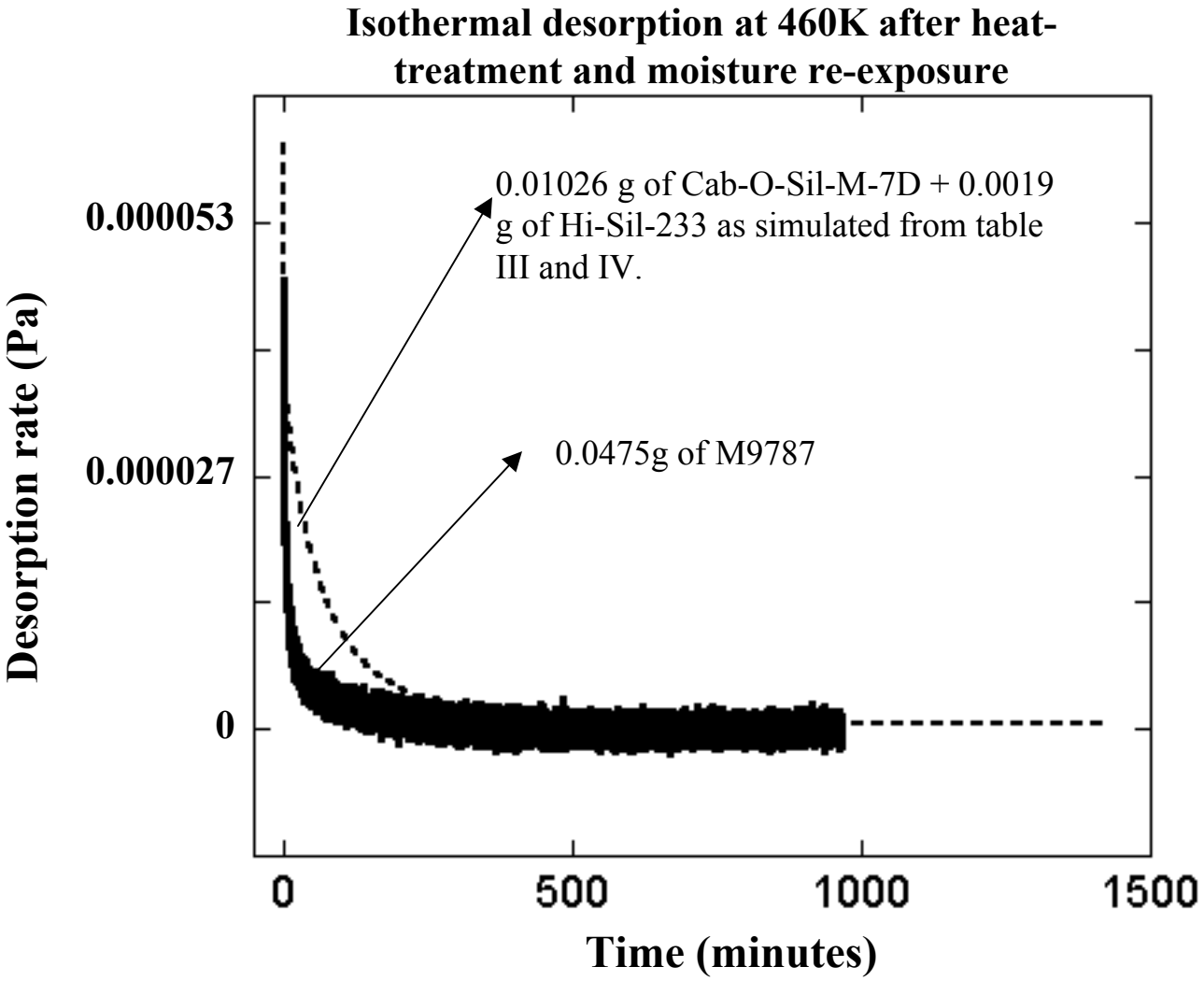
Isothermal desorption at 460K after heat-treatment and moisture re-exposure
0.01026 g of Cab-O-Sil-M-7D + 0.0019 g of Hi-Sil-233 as simulated from table III and IV.
0.0475g of M9787
0.000053
0.000027
0
Desorption rate (Pa)
0
500
1000
1500
Time (minutes)

Fig. 8

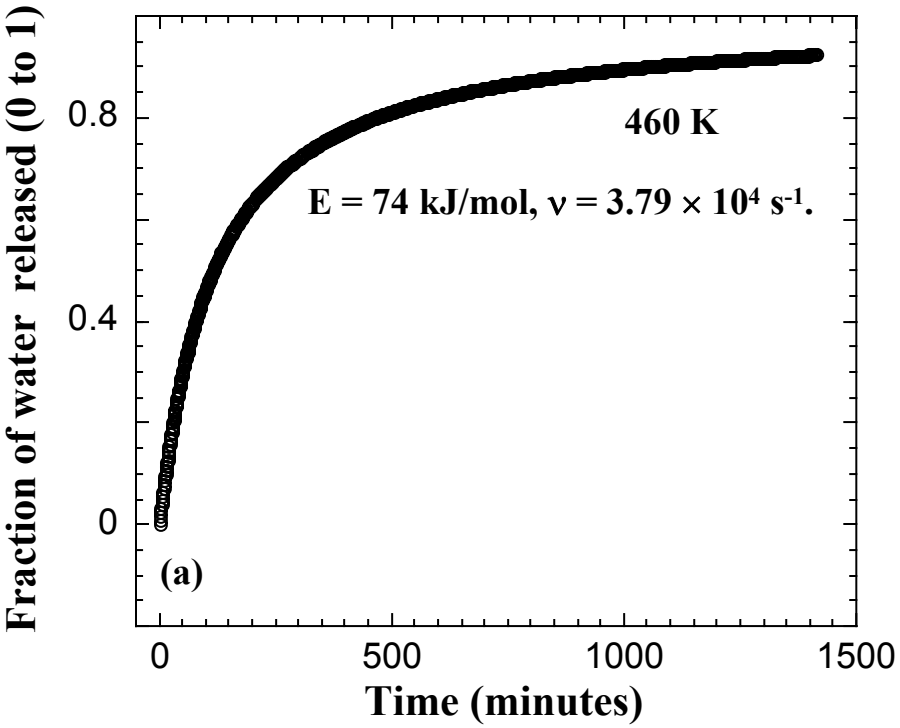
Fraction of water released (0 to 1)
0.8
0.4
0
460 K
E = 74 kJ/mol, ν = 3.79 × 10⁴ s⁻¹.
(a)
0
500
1000
1500
Time (minutes)

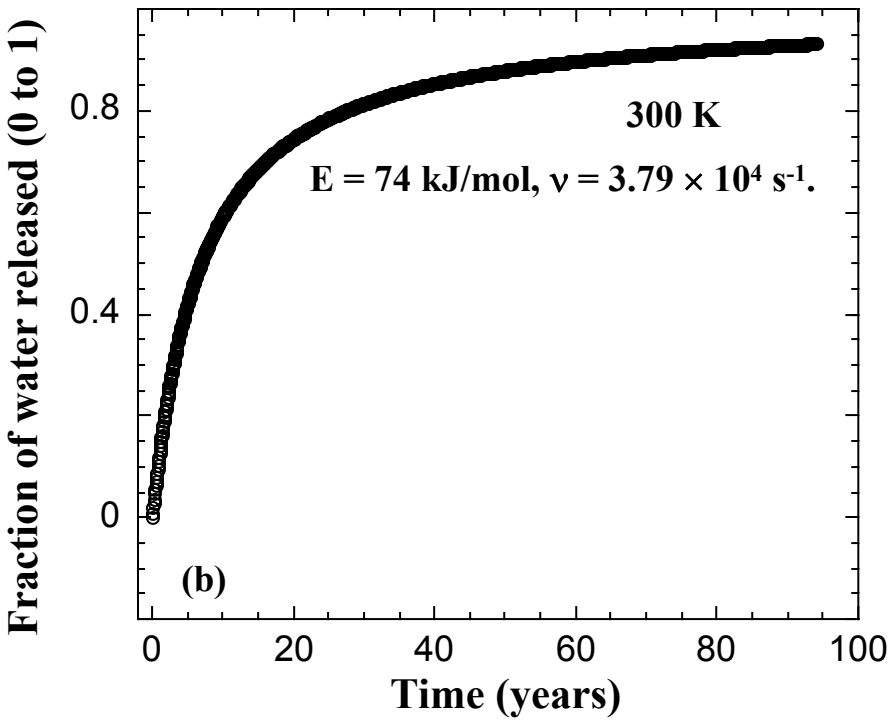
Fraction of water released (0 to 1)
0.8
0.4
0
300 K
E = 74 kJ/mol, ν = 3.79 × 10⁴ s⁻¹.
(b)
0
20
40
60
80
100
Time (years)

Fig. 9

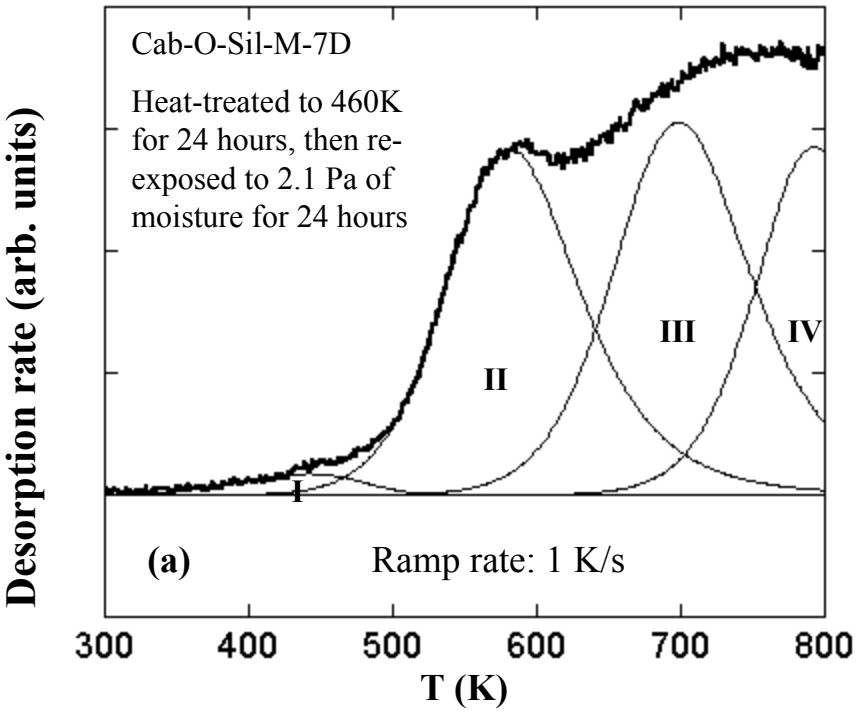
Cab-O-Sil-M-7D
Heat-treated to 460K for 24 hours, then re-exposed to 2.1 Pa of moisture for 24 hours
I
II
III
IV
(a)
Ramp rate: 1 K/s
Desorption rate (arb. units)
300
400
500
600
700
800
T (K)

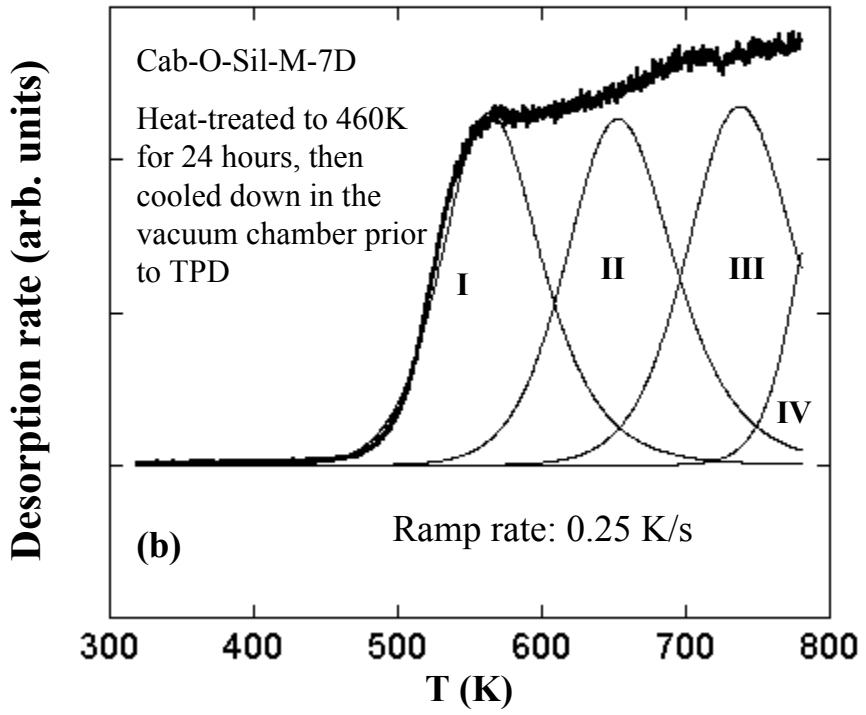
Cab-O-Sil-M-7D
Heat-treated to 460K for 24 hours, then cooled down in the vacuum chamber prior to TPD
I
II
III
IV
(b)
Ramp rate: 0.25 K/s
Desorption rate (arb. units)
300
400
500
600
700
800
T (K)

Fig. 10

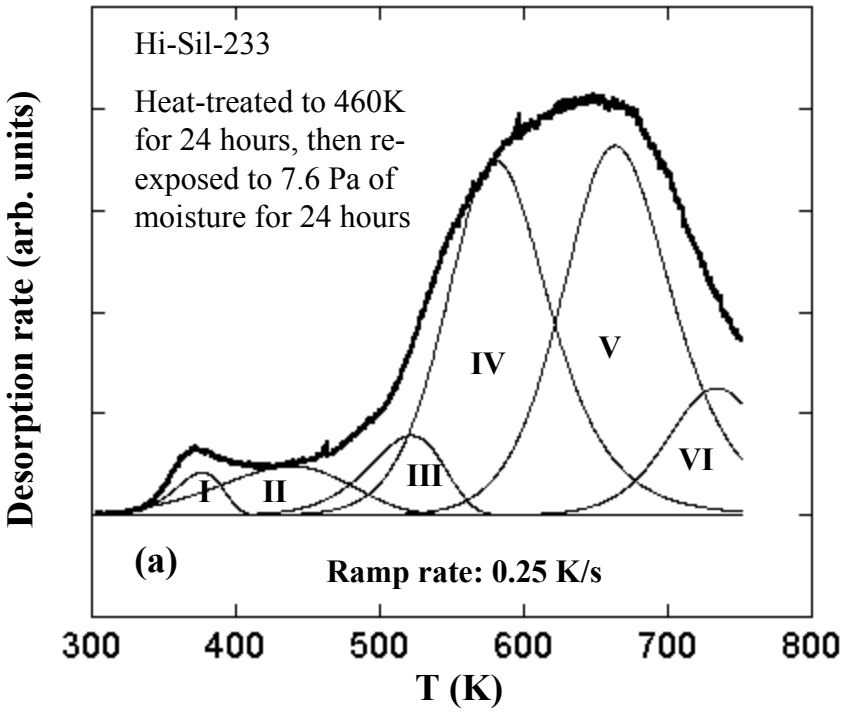
Hi-Sil-233
Heat-treated to 460K for 24 hours, then re-exposed to 7.6 Pa of moisture for 24 hours
Desorption rate (arb. units)
I
II
III
IV
V
VI
(a)
Ramp rate: 0.25 K/s
300
400
500
600
700
800
T (K)

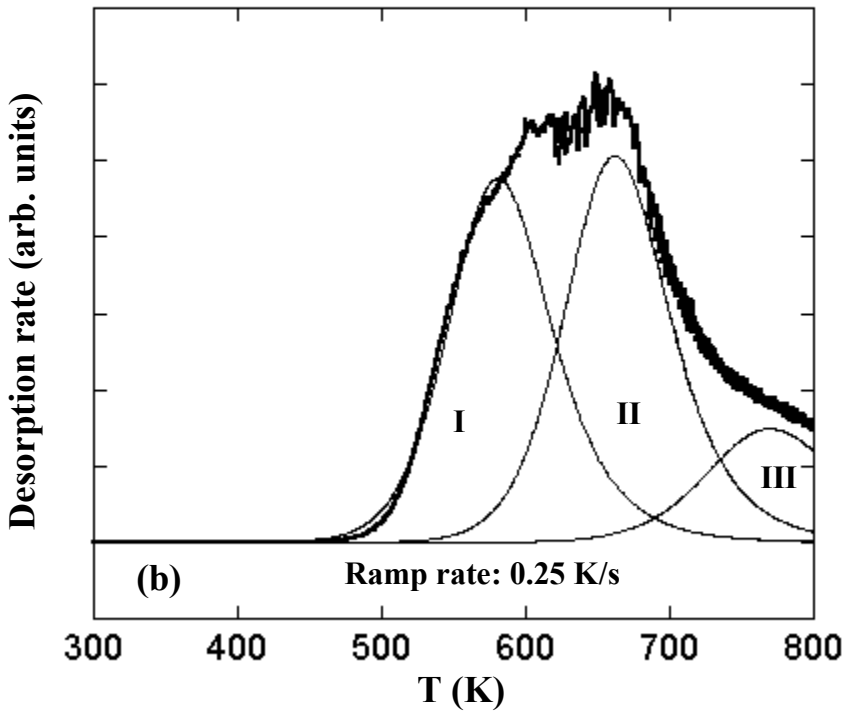
Desorption rate (arb. units)
I
II
III
(b)
Ramp rate: 0.25 K/s
300
400
500
600
700
800
T (K)

Fig. 11

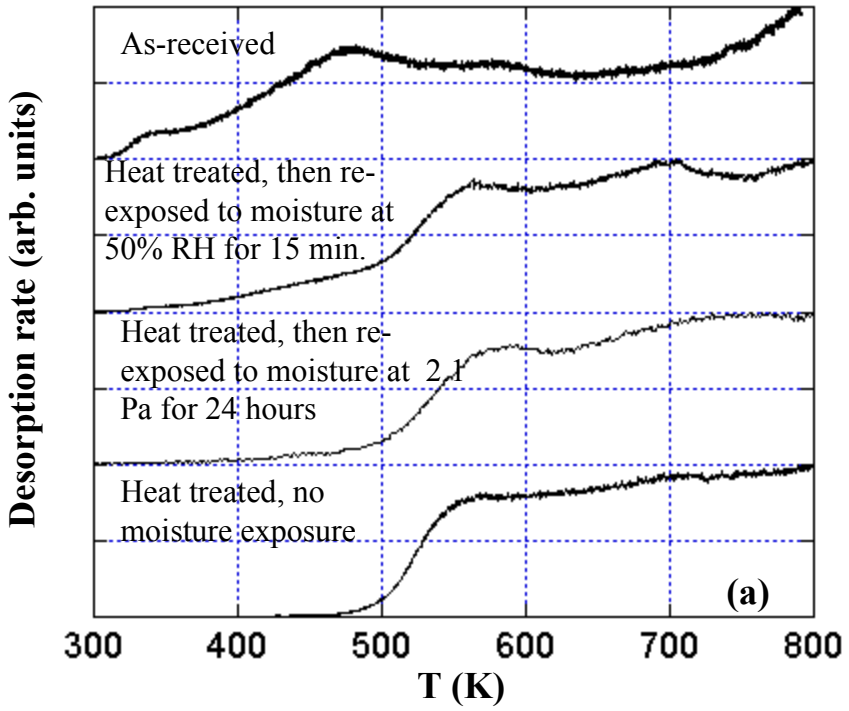
As-received
Heat treated, then re-exposed to moisture at 50% RH for 15 min.
Heat treated, then re-exposed to moisture at 2.1 Pa for 24 hours
Heat treated, no moisture exposure
(a)
Desorption rate (arb. units)
300
400
500
600
700
800
T (K)

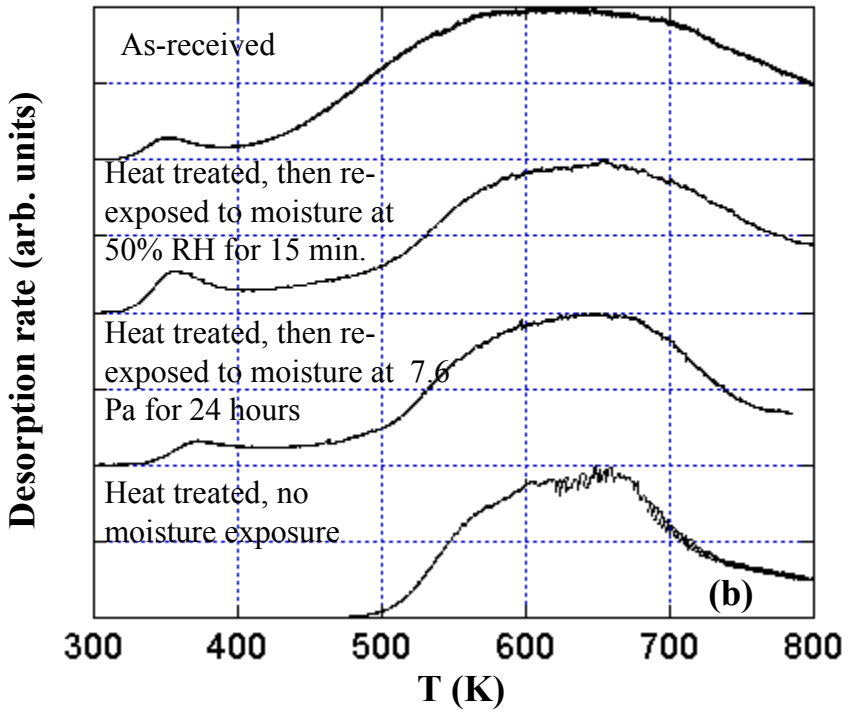
As-received
Heat treated, then re-exposed to moisture at 50% RH for 15 min.
Heat treated, then re-exposed to moisture at 7.6 Pa for 24 hours
Heat treated, no moisture exposure
(b)
Desorption rate (arb. units)
300
400
500
600
700
800
T (K)

Fig. 12

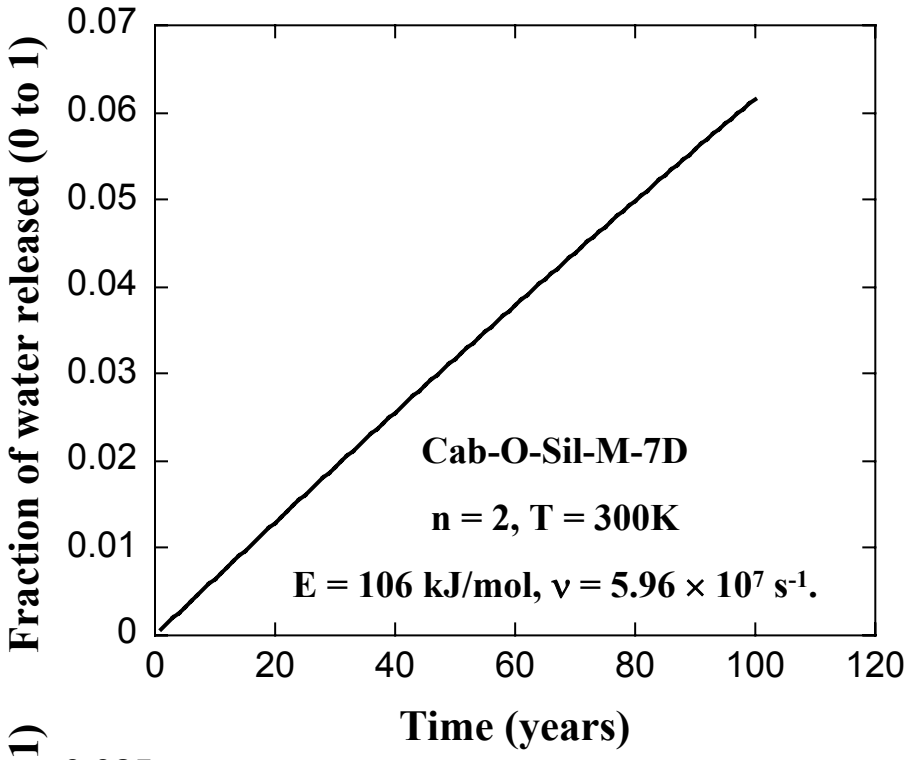
Fraction of water released (0 to 1)
0.07
0.06
0.05
0.04
0.03
0.02
0.01
0
0
20
40
60
80
100
120
Time (years)
Cab-O-Sil-M-7D
n = 2, T = 300K
E = 106 kJ/mol, ν = 5.96 × 10^7 s^-1.

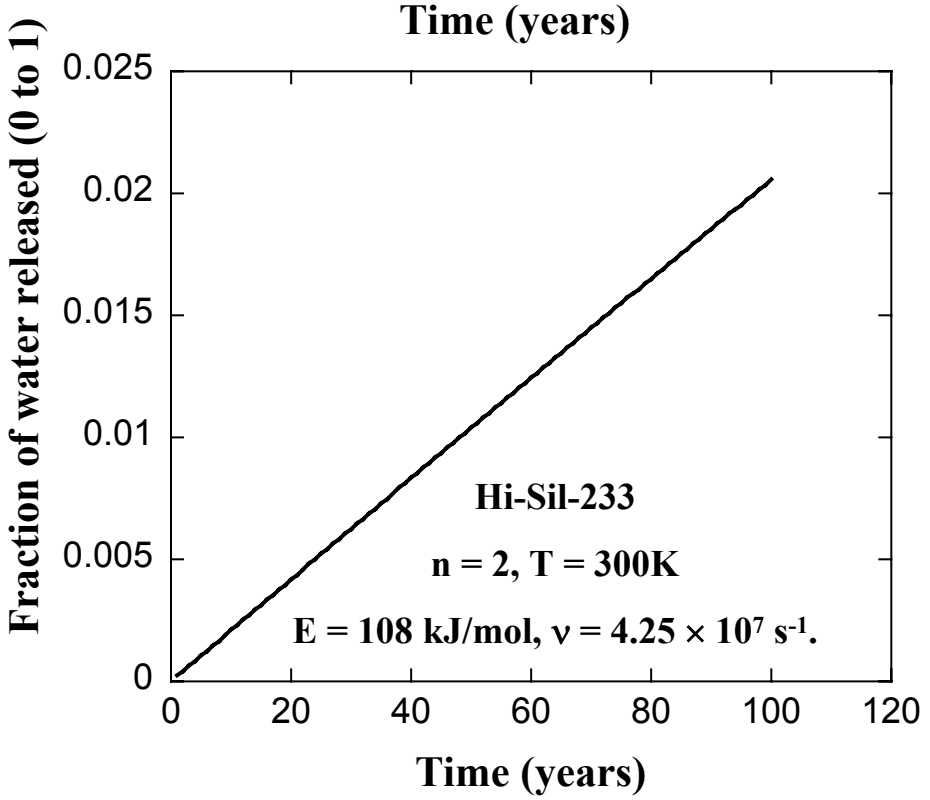
Fraction of water released (0 to 1)
0.025
0.02
0.015
0.01
0.005
0
0
20
40
60
80
100
120
Time (years)
Hi-Sil-233
n = 2, T = 300K
E = 108 kJ/mol, ν = 4.25 × 10^7 s^-1.

Fig. 13